Available online at www.sciencedirect.com
SCIENCE DIRECT®
ELSEVIER
Solid State Communications 137 (2006) 585–588
solid state communications
www.elsevier.com/locate/ssc

Interconnected β-Ni(OH)$_2$ sheets and their morphology-retained transformation into mesostructured Ni

Xiaomin Ni, Qingbiao Zhao, Beibei Li, Jing Cheng, Huagui Zheng *

Department of Chemistry, University of Science and technology of China, Hefei, Anhui 230036, People's Republic of China

Received 16 June 2005; received in revised form 15 January 2006; accepted 19 January 2006 by B. Jusserand

Abstract

A facile route was described for the synthesis of interconnected β-Ni(OH)$_2$ sheets, which was realized by thermal treatment of $Ni(NH_3)_6^{2+}$ solution at 95 °C. X-ray diffraction (XRD), transmission electron microscopy (TEM), field emission scanning electron microscopy (FE-SEM), infrared absorption spectrum (IR) and Raman spectrum were used to characterize the product. The complexation of ammonia and temperature played important roles for the formation of the assembled structure. Thus-prepared β-Ni(OH)$_2$ were morphology-retained transformed into mesostructured Ni by further reduction in H_2 current for 1.5 h.

PACS: 61.66.Fn; 68.55.Jk; 83.80.Pc

Keywords: B. Chemical synthesis; B. Crystal growth; C. Scanning and transmission electron microscopy

1. Introduction

Morphology always greatly affected the properties and applications of materials [1]. Various fields, such as electron conduction, diagnosis, catalysis and nanodevices all press for materials with special shapes. Recently, the construction of assembled structures has become a major issue for their unique applications which could not be achieved by their discrete or bulk counterparts [2–5]. In general, fabrication of assembled structure depends on the molecule interactions between the surfactants or polymers which were absorbed on the surface of subunits. For instances, smecticlike arrays of Te nanorods were driven by the van der Waals forces among the surfactant molecules on particle surfaces; spherical aggregates of monolayer polymer-protected gold nanoparticles were prepared through hydrogen-bonding interactions; assembly of magnetite nanoparticles were achieved in the presence of ternary surfactant combinations [6–8]. However, these techniques most often require special instruments, restricted experimental conditions and delicate know-how. Moreover, the aggregated structures are easy to collapse if the templates were removed, resulting in the difficulty in assembling them into nanodevices. It is still challenging to develop simple routes for the generation of assembled structures.

β-Ni(OH)$_2$ is an important positive electrode active material in rechargeable Ni-based alkaline batteries, and metallic nickel shows various applications in magnetic recording, catalysis, and conduction [9,10]. Owing to that shape, properties and applications of materials are intrinsically linked, exploitations of different shaped materials have been a focus research theme. To date, a few different shapes of β-Ni(OH)$_2$ other than isotropic nanoparticles have been fabricated, such as nanosheets, nanorods, pancakes, microtubes [11–14]. As for nickel, hollow spheres, nanobelts and nanowires, nanotubes, nanorods and hexagonal sheets all have been prepared [15–19]. However, to the best of our knowledge, there have not been seen any reports on the synthesis of assembled structure of β-Ni(OH)$_2$ and Ni up to date.

Herein, we introduced a simple route for the creation of interconnected β-Ni(OH)$_2$ sheets by hydrothermal treating nickel ions in ammonia solution at 95 °C. In addition, by reduction of thus-prepared β-Ni(OH)$_2$ in H_2 current at 500 °C for 1.5 h, assembled mesostructure of metallic Ni was produced, inheriting the morphology of β-Ni(OH)$_2$ precursor.

2. Experimental

All the reagents were analytic purity. In a typical experiment, 0.4 mmol $NiCl_2 \cdot 6H_2O$ was dissolved into 35 ml

---

* Corresponding author. Tel.: +86 551 3606144; fax: +86 551 3601600.
E-mail address: hgzheng@ustc.edu.cn (H. Zheng).

0038-1098/$ - see front matter © 2006 Elsevier Ltd. All rights reserved.
doi:10.1016/j.ssc.2006.01.033

distilled water to give a green transparent solution. Then 5 ml ammonia solution (28 wt%) was added under magnet stirring and the solution turned blue, indicating the complexation of Ni^{2+} and ammonia. The mixture was transformed into a 50 ml Teflon-lined autoclave, sealed and maintained at 95 °C for 4 h. After the heating treatment was completed, green powder was found deposited on the wall of the clave. The product was collected and rinsed, and finally dried in a vacuum at 105 °C for 4 h (sample 1). Part of the dried powder was heated in H_2 current (30 ml min^{-1}) at 450 °C for 1.5 h in a fixed-bed reactor, and further kept in H_2 current until the temperature was decreased to room temperature (sample 2).

X-ray diffraction (XRD) patterns of the samples were recorded on a Philips X'pert diffractometer with Cu Kα radiation ($\lambda = 1.54178$ Å). Morphology of the samples were studied with transmission electron microscope (TEM, Hitachi, H-800) with an accelerating voltage of 200 kV, field emission scanning electron microscopy (FSEM, JEOL JSM-6300F). Infrared absorption (IR) spectrum was performed with a Nicolet FT-IR-170 SX spectrometer at room temperature. The Raman spectrum was collected at ambient temperature on a SPEX 1403 spectrometer with an argon-ion laser at an excitation wavelength of 514.5 nm.

3. Results and discussion

Fig. 1(a) gave the XRD patterns of the sample 1, which was assigned to the obtained β-$Ni(OH)_2$. No peaks of α-$Ni(OH)_2$ or nickel oxides were detected, indicating pure product was generated under current experimental conditions. Compared with the standard pattern of β-$Ni(OH)_2$ (JCPDS 74-2705), the peak intensity of (00l) was sharply strengthened.

Morphology of the sample was studied with FE-SEM and TEM. A typical low-magnification image in Fig. 2(a) shown that as-prepared β-$Ni(OH)_2$ was film-like. The corresponding magnified image in Fig. 2(b) shown that the film comprised sheet-like crystals with a size of 50–100 nm in thickness and 0.3–1.0 μm in side length. A section image detailed that the sheets were aligned vertically with a height of about 3.0 μm, as seen in Fig. 2(c). Thus-prepared structure was found very firm and long-time ultrasonication could not destroy it. During the TEM studies, only a few detached sheets were observed. Two typical hexagonal sheets with a diameter of 0.4–1.0 μm were shown in the image inset in Fig. 2(d) and the corresponding ED pattern demonstrated that the sheets were single crystalline. According to the diffraction dots, the basal surface of the sheets could be indexed as the {0001} planes. ED patterns recorded on the different individual sheet were essentially the same, indicating that all the sheet-like subunits possessed the same crystallographic character. Considering their special assembling manner, the intensified (001) peak of Fig. 1(a) could be ascribed to the non-random average orientation of the platelet subunits.

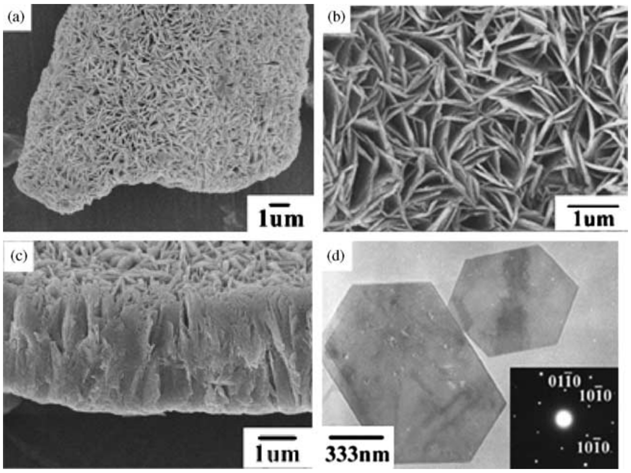

Fig. 2. FE-SEM image of the β-$Ni(OH)_2$ sample: (a) a low-magnification image; (b) a high-magnification image; (c) FE-SEM image of a section of the self-assembled structure; (d) a typical TEM image and corresponding and the corresponding ED pattern of two discrete hexagonal nickel sheets.

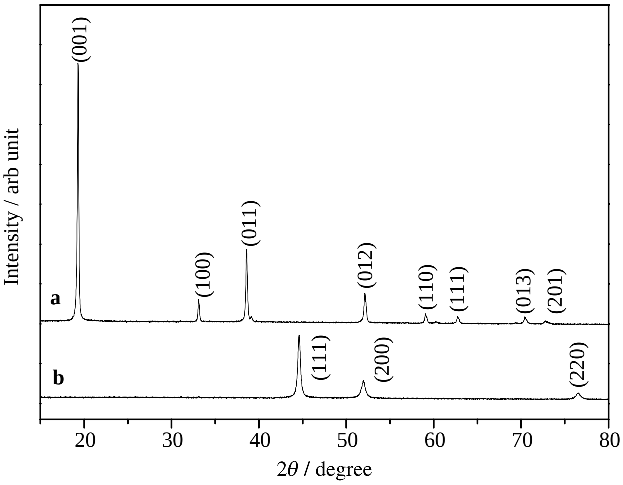

Fig. 1. XRD patterns of the two samples. (a) The obtained β-$Ni(OH)_2$; (b) the sample of Ni.

Fig. 3 gave a typical IR spectrum of the resulted β-$Ni(OH)_2$. A narrow and sharp peak at 3650 cm^{-1} was owing to the ν (OH) stretching vibration, which confirmed the β-$Ni(OH)_2$ phase of the product [20]. The strong band at 527 cm^{-1}

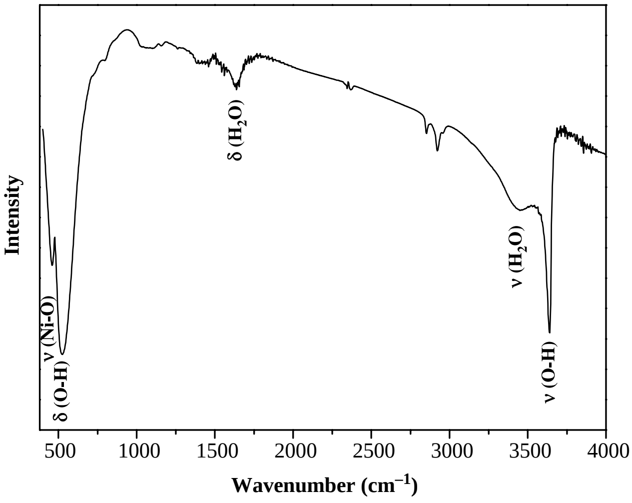

Fig. 3. IR spectrum of as-prepared β-$Ni(OH)_2$ sample.

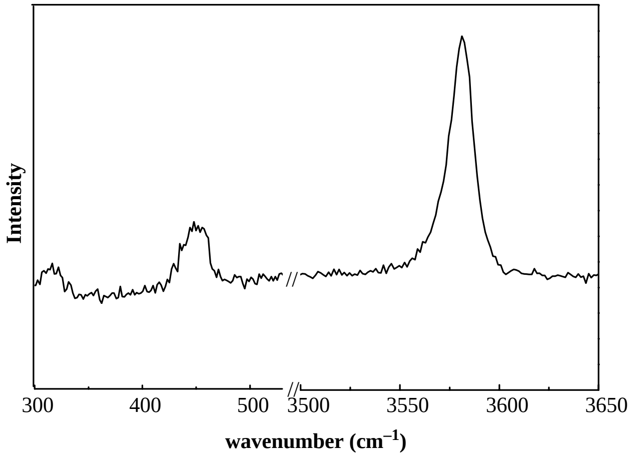

Fig. 4. Raman spectrum of as-prepared β-$Ni(OH)_2$ sample.

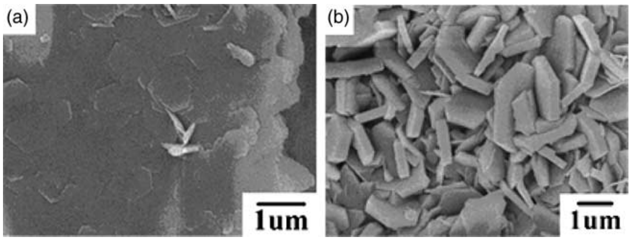

Fig. 5. SEM images of the sample obtained at different temperature: (a) 80 °C. (b) 110 °C.

corresponded to the lattice vibration δ (OH) of hydroxyl groups [20]. Peaks at 3440 and 1641 cm^{-1} resulted from the ν (H_2O) stretching vibration and δ (H_2O) bending vibration of water molecules, which were absorbed on the product. A small weak peak centered around 460 cm^{-1} was assigned to the Ni–O stretching mode [21].

Raman spectrum of the product was given in Fig. 4. Two small peaks located at 317.0 and 446.8 cm^{-1}, together with a strong sharp peak at 3581.1 cm^{-1} emerged, which were consistent with the reported values of crystalline β-$Ni(OH)_2$ [22]. The absence of the peak centered around 510 cm^{-1} indicated the nice crystallization of the product with few proton vacancies and stacking faults [23].

Interestingly, in the experiment we found that most of the green product was deposited on the wall of the claves and little powder was collected from the solution. It was shown that the product was practically the film of β-$Ni(OH)_2$ which grew directly on the Teflon matrix of the clave. However, in previous reports dispersive nanorods and nanosheets of β-$Ni(OH)_2$ were fabricated by a similar reaction using ammonia as complexing agents and alkali source [11,12]. But we noted that the temperature in their experiments was much higher to 180 and 200 °C. Meanwhile, the concentrations of nickel source were about 8 and 17 times higher than that of our system, respectively. Based on investigations on the effect of the experimental conditions, we found that the lower temperature was of great importance for the formation of our self-assembled structure, while the concentration of nickel source did not show obvious influence. In the current system, generation of $Ni(OH)_2$ could be could be formulated as the reaction: $Ni(NH_3)_6^{2+} + 2H_2O \rightarrow Ni(OH)_2\downarrow + 2NH_4^+ + 4NH_3$. When heating, the ammonia decomplexation occurred for the sharp decrease of the complexation constant, resulting in the generation of $Ni(OH)_2$ particles. The presence of ammonia and the low temperature made the reaction process at a relatively slow rate [24]. As the surface of the wall of the clave was not absolutely smooth and due to temperature gradient from the wall to the inside, the generated nickel hydroxide would preferentially nucleate on the active sites of the wall. Due to its intrinsic brucite-type structure and the complexation of ammonia, in the following growth stage, these nuclei gradually developed into interconnected sheets with the newly produced $Ni(OH)_2$ continuously feeding [25]. Of course, the nucleation and growth of particles in solution was inevitable which emerged as flowerlike microparticles [13]. As the perfectness of thin films is related to the reaction rate, at different temperatures the obtained films exhibited different details [26]. Keeping other reaction conditions same, lowing the temperature to 80 °C resulted in much larger flakes with several thin hexagonal sheets lying on the surface (Fig. 5(a)). While at a higher temperature of 110 °C, films with thicker hexagonal sheets protrudent emerged, as seen in Fig. 5(b). It indicated that the temperature affected the growth rates of the basal and edge faces of the $Ni(OH)_2$ plates. A higher temperature facilitated the growth of edge surface, while the lower temperature favored the development of the basal surfaces. However, thermal dependence of the surface energies of the basal and edge faces of the sheets was still not unknown and a more deeply research was underway. As for the disordered aggregation of the sheets in Fig. 5(b), it was possibly attributed to the faster reaction rate at higher temperature which was not favorable for their ordered assembly.

We further tried to transform the assembled structure of β-$Ni(OH)_2$ into metallic nickel by hydrogen reduction. XRD pattern in Fig. 1(b) revealed that the obtained black powder was face-centered cubic (fcc) nickel (JCPDS 4-850). No characteristic peaks of hydroxides or oxides were detected. FE-SEM images in Fig. 6 revealed the resulted nickel powder possessed a mesoporous skeleton consisted of interconnected particles, approximately maintaining the size and the assembled shape the precursor. However, the former compact sheets became porous, which may be resulted from the release of H and O atoms during the thermal reduction. New properties including catalysis or conduction are expected to be found in this mesostructured nickel.

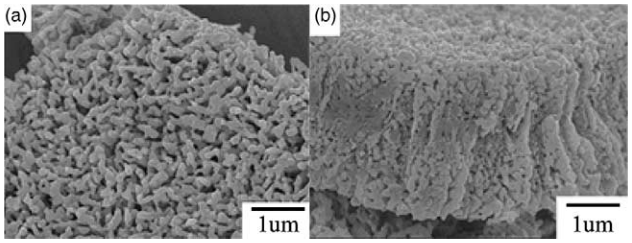

Fig. 6. FE-SEM image of the Ni sample: (a) image of the top surface of the self-assembled structure; (b) image of a section of the self-assembled structure.

4. Conclusion

In conclusion, a new kind of assembled β-$Ni(OH)_2$ structure was produced through a simple hydrothermal treatment of nickel chloride using ammonia as complexing agent. The complexation of ammonia and the low temperature were found play important roles for the formation of this special morphology. By further reducing the obtained β-$Ni(OH)_2$ powder in H_2 atmosphere, skeleton-like Ni consisted of porous sheets were created, maintaining the shape of the precursor. Such assembled structures of β-$Ni(OH)_2$ and Ni are expected to be fabricated on other substrates and the relative work is in progress.

Acknowledgements

The authors are grateful to the transmission electron microscopy and field emission scanning electron microscopy facilities of Structure Research Laboratory of University of Science and Technology of China for assistance.

References

[1] B. Wiley, Y. Sun, Y. Xia, Langmuir 21 (2005) 8087.
[2] Y. Wu, H. Yan, M. Huang, B. Messer, J.H. Song, P. Yang, Chem. Eur. J. 8 (2002) 1260.
[3] M. Bruchez, M. Moronne, P. Gin, S. Weiss, A.P. Alivisatos, Science 281 (1998) 2013.
[4] E.V. Shevchenko, D. Talapin, A.L. Rogach, A. Kornowski, M. Haase, H. Weller, J. Am. Chem. Soc. 124 (2001) 11480.
[5] S. Sun, C.B. Murray, D. Weller, L. Folks, A. Moser, Science 287 (2000) 1989.
[6] Z. Liu, Z. Hu, J. Liang, S. Li, Y. Yang, S. Peng, Y. Qian, Langmuir 20 (2004) 214.
[7] A.K. Boal, F. Ilhan, J.E. Derouchey, T. Thurn-Albercht, T.P. Russell, V.M. Rottello, Nature 404 (2000) 746.
[8] Y. Hou, S. Gao, T. Ohta, H. Kondoh, Eur. J. Inorg. Chem. 4 (2004) 1169.
[9] H.M. French, M.J. Henerson, A.R. Hillman, E. Vieil, J. Electroanal. Chem. 500 (2001) 192.
[10] D.H. Chen, C.H. Hsieh, J. Mater. Chem. 12 (2002) 2412.
[11] Z.H. Liang, Y.J. Zhu, X.L. Hu, J. Phys. Chem. B 108 (2004) 3488.
[12] J. Liang, Y. Li, Chem. Lett. 32 (2003) 1126.
[13] C. Coudun, J.F. Hochepied, J. Phys. Chem. B 109 (2005) 6069.
[14] F.S. Cai, G.Y. Zhang, J. Chen, X.L. Gou, H.K. Liu, S.X. Dou, Angew. Chem. 116 (2004) 4308.
[15] J. Bao, C. Tie, Z. Xu, Q. Zhou, D. Shen, Q. Ma, Adv. Mater. 13 (2001) 1631.
[16] Z. Liu, S. Li, Y. Yang, S. Peng, Z. Hu, Y. Qian, Adv. Mater. 15 (2003) 1946.
[17] J. Bao, Y. Liang, Z. Xu, L. Si, Adv. Mater. 15 (2003) 1832.
[18] N. Coydente, M. Respaud, F. Secocq, M.J. Casanove, C. Amiens, B. Chaudret, Nano Lett. 1 (2001) 565.
[19] X. Ni, L. Cheng, H. Zheng, D. Zhang, Q. Zhao, J. Song, Chem. Lett. 33 (2004) 1564.
[20] P.V. Kamath, G.N. Subbanna, J. Appl. Electrochem. 2 (1992) 478.
[21] G.J. de, A.A. Soler-Illia, M. Jobbagy, A.E. Regazzoni, M.A. Blesa, Chem. Mater. 11 (1999) 3140.
[22] M. Rajamathi, P.V. Kamath, R. Seshadri, J. Mater. Chem. 10 (2000) 503.
[23] K. Robert, M. Frank, J. Electrochem. Soc. 144 (1997) 485.
[24] Y.D. Li, C.W. Li, H.R. Wang, L.Q. Li, Y.T. Qian, Mater. Chem. Phys. 59 (1999) 88.
[25] A.D. Vidal, B. Beaudoin, N.S. Epée, M.T. Elhsissen, A. Audemer, M. Figlarz, Solid State Ionics 84 (1996) 239.
[26] S.C. Davis, K.J. Klabunde, Chem. Rev. 82 (1982) 157.